Optimising the hydrophobicity of sands by silanisation and powder coating

Abstract

Sands are naturally hydrophilic granular materials, yet, rendering them hydrophobic could lend them to a wide range of geotechnical applications. This study describes a powder coating procedure performed after chemically modifying the surfaces of coarse, medium and fine sands and examines its effect on their hydrophobicity. The purpose is to render these granular materials more hydrophobic than what is conventionally achieved by chemical methods using a simple technique. The procedure consists of first silanising both the sands and silica powder at a similar concentration by means of an organosilane to modify their surface chemistry, then the silica powder is adhered to the sands at a mass mixing ratio to alter their hydrophobicity. Irrespective of the concentrations and mixing ratios, the powder coating procedure enhances the hydrophobicity of sands in comparison to the sole use of the chemical method. Changes in the morphology of the sand grains, such as their particle size, particle shape and surface roughness resulting from the powder coating procedure are examined by means of dynamic image analysis, profilometry and scanning electron microscopy. The effects of surface chemistry, surface roughness and air on the hydrophobicity of the sands are discussed based on theoretical wetting models to analyse the experimental results.

Keywords

Chemical properties; laboratory tests; particle-scale behavior; sands; ground improvement

List of notations

CA	contact angle
γ_{wa}	interfacial force between the water-air
γ_{sw}	interfacial force between the solid-water
γ_{sa}	interfacial force between the solid-air
θ_y	Young's contact angle
θ_w	Wenzel's contact angle
r	roughness factor
θ_{cb}	Cassie-Baxter's contact angle
f_1	area fraction of the solid in contact with the water drop
k^{-1}	capillary length of water
ρ	density of water
g	gravitational constant
H	water entry pressure
r_c	capillary radius
DMDCS	dimethyldichlorosilane
PDMS	polydimethylsiloxane
DIA	dynamic image analyser
D_{50}	median value of cumulative distribution for particle size
S_{50}	median value of cumulative distribution for sphericity
Ar_{50}	median value of cumulative distribution for aspect ratio
CV_{50}	median value of cumulative distribution for convexity
SEM	scanning electron microscope
R_a	surface roughness
C	critical concentration of the silica powder

1. Introduction

Rendering soil particles hydrophobic by mixing with chemical additives is known to reduce the expansion of swelling clays (Hernandez *et al.* 2005), influence the capillary rise in fine silt (Orozco and Caicedo, 2017) and in sands, to alter their electrical conductivity (Dong and Pamukcu, 2015) and their evaporation rate (Kim *et al*. 2015). With sands, hydrophobisation can also lead to several geotechnical applications, as barriers at the soil–atmosphere–vegetation and at soil–structure interfaces. For example, their potential use in solid waste landfills as covers to prevent water infiltration has been proposed by Subedi *et al*. (2012). The efficiency of using hydrophobic sands for such a system will depend on the water entry pressure i.e. the critical pressure at which water displaces air, which is a function of the sand properties such as porosity (Lee *et al*. 2015) and is positively correlated to the extent of hydrophobicity (Carillo *et al*. 1999). The water entry pressure, H is related to the contact angle (CA) according to equation (1) where γ_{wa} is the interfacial force between the water-air phases, r_c is the capillary radius, g is the gravitational constant and ρ, the density of water. Furthermore, hydrophobicity in sands also influences their water retention properties (Keatts *et al*. 2018). Key advantages for using hydrophobic sands are as follows: 1) High gas permeability while remaining impermeable to liquids. 2) Volumetric stability, unlike clays that are prone to swelling and shrinking (including desiccation cracks). 3) Reusing waste–derived materials such as glass for hydrophobisation.

$$H = \frac{2\gamma_{wa}\cos CA}{r_c g \rho} \quad (1)$$

Hydrophobic materials, characterised by a CA > 90° have found applications in numerous fields as microfluidics devices, self-cleaning surfaces and textile fabrics (Grunze, 1999; Blossey, 2003; Zimmermann *et al*. 2008). On a flat surface, hydrophobicity is exclusively a function of the surface chemistry, with surfaces treated with fluoropolymers being the most hydrophobic (Lafuma and Quéré, 2003; Darmanin and Guittard, 2015); the CAs reported on these surfaces do not exceed 120°. On rough surfaces, the surface texture has been shown to contribute to hydrophobicity (Wenzel, 1936; Lafuma and Quéré, 2003). A commonly cited example throughout the literature is the lotus leaf, displaying multi-scales of roughness, conducive to a

high CA of 150°–160° (Feng *et al*. 2002; Darmanin and Guittard, 2015). Numerous experimental studies have been devoted to functionalising materials using both chemical and physical methods such as altering their surfaces by microscale (e.g. using silicon pillars) and nanoscale (e.g. using carbon nanotubes) modifiers to achieve high CAs, comparable to the lotus leaf (Shirtcliffe *et al*. 2004; Wang *et al*. 2007; Zhang *et al*. 2015). However, adapting such physical modifications to granular materials such as sands is not feasible due to the costs involved. Therefore, for applications to geotechnical problems, user-friendly approaches that take into account economic factors are needed. A new method is introduced in this paper to optimise the hydrophobicity of sands through comparatively simple techniques. A brief overview of the methods currently used to render granular soils hydrophobic is first given below.

Chemical methods to render sands hydrophobic include the use of agents such as fatty acids (Subedi *et al*. 2012), waxes (Bardet *et al*. 2014), oils (Zhang *et al*. 2016) and organosilanes (Ng and Lourenço, 2016). From a sample preparation perspective, mixing organosilanes in liquid form with sands, being a single step process is the most straightforward and also a well-documented method that has been shown to induce hydrophobicity in sands while also retaining their non-biodegradability in water (Bachmann and McHale, 2009). Organosilanes can be broadly classified as mono–functional (e.g. trimethylchlorosilane) and multi–functional (e.g. dimethyldichlorosilane and octadecyltrichlorosilane). Mono-functional organosilanes have a single reactive site which can react with only one hydroxyl group (–OH) on the sands whereas the reaction between multi-functional organosilanes and sands lead to complex molecular configurations as a result of both vertical and horizontal polymerisations (Tripp and Hair, 1991). A comparison between different organosilanes used to hydrophobise sands was investigated by Chan and Lourenço (2016). They concluded that the use of multi-functional organosilanes such as dimethyldichlorosilane (DMDCS) required lesser amount of chemical and thus was more cost effective to achieve the maximum CA. The synthesis of hydrophobic sands using organosilanes is known as silanisation. With DMDCS, the basic mechanism first involves reaction with water (present in the atmosphere and/or on the sands) to give polydimethylsiloxane (PDMS) which is a soft polymeric coating (Liu *et al*. 2019) and hydrogen chloride according to equation (2) where *n* is the number of DMDCS repeating units. The hydroxyl groups on the sands then react with

PDMS to yield outward-oriented methyl groups (-CH_3) responsible for hydrophobicity (Goebel *et al*., 2007).

$$n[(CH_3)_2SiCl_2] + n[H_2O] \rightarrow [(CH_3)_2O]_n + 2nHCl \quad (2)$$

Physical methods to optimise the hydrophobicity of sands are designed based on particle characteristics such as particle size, particle shape and surface roughness. They are typically not used on their own, but combined with chemical treatment of the soil grains. The dependency of the hydrophobicity of soils on particle size has been shown in several studies such as Bachmann *et al*. (2003) with the finer fractions exhibiting a larger CA than the coarser ones while Saulick *et al*. (2018) showed that for a given surface chemistry of granular materials comprising of sands and artificial particles synthesised with DMDCS, angular particles were more hydrophobic. With granular materials, two scales of surface roughness can be defined, namely the surface roughness of single particles as investigated by Yang *et al*. (2016) and the surface roughness of a series of particles, quantified by Saulick *et al*. (2018) as a function of both particle size and particle shape. The latter have shown that for a given surface chemistry of granular materials, the finer and more angular-shaped particles translate into a smaller surface roughness parameter and are more hydrophobic.

The research in this paper presents a new method for optimising or controlling the hydrophobicity of sands by combining chemical treatment by means of an organosilane (chemical method) and surface alteration by powder coating (physical method) in order to render them more hydrophobic than what is conventionally achieved by chemical methods. Techniques comprising dynamic image analysis, scanning electron microscopy and optical interferometry were used to characterise the morphology of the grains before and after powder coating. Although the methods used, individually or combined are known to influence considerably the CAs of sands, the combined effect of chemically and physically modifying their surfaces on hydrophobicity has not been investigated to date. To achieve this aim, sands of different grading were first chemically modified at different concentrations and then physically altered by powder coating at different mixing ratios. The results were compared to sands that

were only chemically modified and any differences in hydrophobicity attributed to the powders coated on the sands. The results are then compared with theoretical wetting models used in physical chemistry such as the Wenzel and Cassie-Baxter models which include effects of surface chemistry, surface roughness and air on the hydrophobicity of granular materials, thus giving an insight into the micro-mechanisms underlying sand wettability.

2. Theoretical background

Three main theoretical models exist which describe the wettability of surfaces; they are the Young's model that assumes the surface to be flat, Wenzel's and Cassie-Baxter's models that consider the roughness of the surfaces.

2.1 Wettability of flat surfaces: Young's model

A drop of water deposited on a solid in air will either spread or adopt a spherical cap-like shape depending on the three interfacial forces on it. They are γ_{wa}, γ_{sw} and γ_{sa} corresponding respectively to the interfacial forces between the water-air, solid-water and solid-air phases. At the three-phase point, resolving the interfacial forces horizontally assuming mechanical equilibrium generates a relationship with the CA on the wet side of the water drop, which is a measure of the wettability of the solid (Figure 1a).

For a drop of water on an ideal (smooth, homogenous, inert, insoluble, non-porous and non-deformable) flat solid, a relationship between the interfacial forces and an angle, θ_y can be established where θ_y is defined as Young's contact angle (Young, 1805):

$$\gamma_{wa} \cos\theta_y + \gamma_{sw} = \gamma_{sa} \quad (3)$$

2.2 Wettability of rough surfaces: Wenzel's model

The model developed by Wenzel (1936) takes into account the effect of surface roughness and modifies Young's equation by a material-independent roughness factor, r to give Wenzel's contact angle, θ_w according to the following equation:

$$\cos\theta_w = r\cos\theta_y \quad (4)$$

The quantity *r* in equation (4) is defined as the ratio of actual (including the surface protrusions) and projected areas of the solid. The Wenzel model assumes a complete wetting where a drop of water completely fills the grooves (Figure 1b). Because the value of *r* always exceeds unity, equation (4) implies that for a solid with θ_y less (greater) than the 90° threshold, hydrophobicity will subdue (intensify).

2.3 Wettability of rough surfaces: Cassie-Baxter's model

Cassie-Baxter's model considers a wetting regime where a drop of water deposited on a solid does not fill the grooves completely and has air trapped between the solid and water interface (Figure 1c) which leads to an enhancement in hydrophobicity. This is due to the synergistic decrease in the area fraction of the solid in contact with the water drop (f_1) and increase in the area fraction of air in contact with the water drop (1- f_1). To account for this difference in chemistry, Cassie and Baxter (1944) expressed the contact angle, θ_{cb} as follows:

$$\cos\theta_{cb} = f_1\left(\cos\theta_y + 1\right) - 1 \quad (5)$$

These three models can be used to compare with the contact angles measured in the laboratory to assess their suitability to describe the hydrophobicity of granular materials, while also giving some insight into what controls the wettability of soils. The following section describes the experimental programme, which consisted of changing the surface properties of a quartz sand by chemical treatment (silanisation) and surface alteration (by powder coating), and quantifying the changes in terms of contact angle and surface morphology.

3. Experiments

3.1 Tested materials

Fujian sand, a commercially available sand with a high proportion of silica was used. Silica powder was chosen to coat the sands due to its widespread use in the construction industry for

producing functional cementitious mixtures (Bentz *et al*., 2017). Both the sands and the silica powder were sourced from a quarry located at Xiamen, Fujian, China. After a dry sieve analysis, three sand fractions were isolated based on their particle sizes: coarse sand (600–1180 µm), medium sand (212–300 µm) and fine sand (63–212 µm). The median particle size (D_{50}) of the silica powder was 23 µm. The sands and silica powder were initially washed and oven-dried at 80°C prior to any tests. Microscope slides made of soda lime-silica glass (with comparable chemistry to the sands and silica powder), and of dimensions 76 × 26 mm by 1 mm thick, were used as references for ideal flat solids.

3.2 Silanisation

A liquid-phase silanisation using DMDCS (Acros Organics, Morris Plains, NJ, USA) was carried out to hydrophobise the sands, silica powder and microscope slides. The silanisation reactions were carried out in a fume cupboard at 14 concentrations (defined as the mass ratio of DMDCS added to the sands or the silica powder expressed as a percentage) to identify the critical concentration—the smallest concentration of DMDCS needed to reach the maximum CA. The concentrations used were between 0.00265% and 3.71%. To render the microscope slides hydrophobic, a total of 20 µl of DMDCS was dispensed from a single channel pipette (Pipetman P100 from Gilson®, Villiers-le-Bel, France) and left to react for 24 hours.

3.3 Powder coating procedure

The first step in the powder coating procedure involved isolating the effect of surface chemistry of the sands and the silica powder by carrying out the silanisation at the critical concentration of the silica powder (*C*). Afterwards, the silanised sand and silanised silica powder were mixed at a mass ratio and the excess silanised silica powder discarded. Next, the mixture was washed on a 63 µm mesh. To accelerate the evaporation process and obtain the powder-coated sands, the mixture was oven-dried at 80°C for 16 hours, to avoid thermal degradation of the PDMS coating (Camino *et al*., 2001). The powder-coated sands are a result of the adhesion between the silanised sand and the silanised silica powder. This involves molecular bonding consisting of intermolecular bonds such as Van der Waal forces when the interfaces are brought in contact supplemented by covalent bonds formed at the interfaces as a result of vertical and horizontal

polymerisations (Kinloch, 1980). In addition to these forces, mechanisms such as mechanical coupling have also been reported (e.g. in Brown (2000)) to contribute to adhesion in polymers. A schematic illustration of the powder coating procedure is shown in Figure 2.

Two parameters were investigated when carrying out the powder coating procedure: (i) the concentration at which the sands and the silica powder was silanised. This concentration was increased from *C* to 2*C* and 7*C*, the critical concentration *C* being considered the minimum required to achieve consistent hydrophobicity. (ii) the mass ratio at which the silanised sand and silica powder was mixed. The ratio of silanised sand and silica powder was first set as 1 to 1 and then raised to 1 to 3. A comparison of the CAs obtained with the values predicted with the models including or not surface roughness will then give some insight into the mechanics of soil wettability at the grain scale.

3.4 Contact angle measurement

A goniometer (Drop Shape Analyzer 25, KRÜSS GmbH, Hamburg, Germany) was used to measure the CAs of the materials via the sessile drop method, a method widely used in the soil and material sciences. Sample preparation for each of the granular materials was carried out according to the technique proposed by Bachmann *et al*. (2000) by fixing a monolayer of the granular materials on a microscope slide with double-sided tape attached to it. Ten micro-liters (10 µL) drops of deionised water were placed on each sample using the automatic dispenser of the goniometer and images were obtained from a charged coupled device camera positioned laterally to the samples. To restrict the influence of the shape of the sessile drop on CAs, the gaps between the granular materials should be less than k^{-1}, the capillary length of water (2.7 mm). The capillary length of water is a characteristic length which depends on the interfacial force between the water-air phases (γ_{wa}), density of water (ρ) and the gravitational constant (g) according to equation (6). Because the gaps between the granular materials in this study are less than the capillary length of water, the influence of gravity on the drop shape can be neglected. The tests were carried out in air at a temperature of 24°C and relative humidity of 65%. Although the sessile drop is a commonly used technique to evaluate CAs, their determination retains an element of subjectivity linked for example to the positioning of the

baseline. The semi-automated technique developed by Saulick *et al*. (2017) was applied to evaluate the CAs using ImageJ, an open source image processing software. The mean value of the ten measurements and the corresponding standard deviation on each sample were adopted as the measured data.

$$k^{-1} = \sqrt{\frac{\gamma_{wa}}{\rho g}} \qquad (6)$$

3.5 Characterisation of particle size, shape and surface roughness

The coating of sand grains by DMDCS and powder may alter their size and morphology. These were examined before and after treatment by means of a dynamic image analyser and an interferometer for a quantitative description of size, shape and texture, and by scanning electron microscopy for a qualitative assessment.

A dynamic image analyser (DIA), QICPIC™ (Sympatec GmbH, Clausthal-Zellerfeld, Germany) was used to refine the characterisation of the particle size and obtain the particle shape of the granular materials. The dispersion of the granular materials was carried out by gravity via the GRADIS™ module and the maximum resolution of the lens in the camera was 10 µm. A frame rate of 250 Hz was selected in both modules for the capture of the 2D binary images. Three shape parameters were investigated, namely: sphericity (ratio of the perimeter of a perfect circle to that of the particle), aspect ratio (ratio of the minimum to maximum Feret diameters) and convexity (ratio of area of the particle to its convex area). A median value of the cumulative distribution, defined as the diameter of the particle that 50% of the sample mass is smaller than (D_{50}) was used for the particle size, and for the characterisation of particle shape, the median values of each of the shape parameters (Sp_{50} for sphericity, Ar_{50} for aspect ratio and Cv_{50} for convexity) obtained from the respective cumulative distributions were reported. It was assumed that the number of images analysed in the characterisations of both particle size and shape was large enough such that analysis of additional images would not change the median values.

A scanning electron microscope (SEM, Zeiss Leo 1530 FEG, Jena, Germany) was used to qualitatively investigate the microscopic and nanoscopic surface morphology of the granular materials. The samples were first sputtered with a thin layer (thickness ~ 5 nm) of a Gold-Palladium alloy in the ratio of 3:2 using the BAL-TEC SCD 005 sputter coater. Images were acquired at working distances of 5–10 mm and at an acceleration voltage of 5 kV.

The characterisation of surface roughness was carried out using an optical white light profilometer, Fogale Microsurf 3D, model M3D 3000 (Fogale Nanotech, Nîmes, France). A Mirau interferometric objective lens with standard magnification of 50 × was used to scan 25 randomly selected areas on the silanised and powder-coated sands with optimum lateral and vertical resolutions of 0.184 µm and 3 nm respectively. To account for the differences in particle sizes of the sands, the square–shaped scanned areas were reduced in decreasing order of particle sizes. The scanned areas of the 600–1180 µm, 212–300 µm and 63–212 µm particle sizes were respectively set as 80 × 80 µm, 40 × 40 µm and 35 × 35 µm. The influence of curvature was excluded from all measurements of surface roughness, which was evaluated using the proprietary result viewer software, Fogale 3D Viewer (Version 2006-06) according to the following equation:

$$R_{\mathrm{a}} = \frac{1}{N}\sum_{\mathrm{n}=1}^{N}|R_{\mathrm{n}}| \qquad (7)$$

with R_a representing the center-line average, N corresponding to the total number of pixels in the scanned area and R_n representing the height of each pixel with respect to the baseline.

4. Results and discussion

4.1 Influence of silanisation and powder coating on hydrophobicity

The CAs of the sands and silica powder before silanisation were found to be ~ 10°. Figure 3 illustrates the relationship between concentration of DMDCS and CAs for the coarse sand, medium sand, fine sand and silica powder following the silanisation reactions. Adding DMDCS improves the non-wettability of the soils significantly, the contact angle increasing for all sands

and the silica powder when concentration increased, with a relatively steeper increase for the coarse sand due to the comparatively smaller surface area (dark solid line).The CA eventually plateaued indicating that further increase in CA solely due to changes in surface chemistry was not feasible. The critical concentration of the fine sand, medium sand and the silica powder was found to be 0.53% and that of the coarse sand was 0.0795%. At the relevant critical concentrations, the CAs of the coarse, medium and fine sands were 109°, 122° and 127° respectively. These granular materials were more hydrophobic than the silanised microscope slides (103°) and less than the silanised silica powder at the critical concentration (137°).

For the powder-coated sands, both the sands and the silica powder were initially silanised at 0.53% (*C*) and mixed at a 1 to 1 mass ratio. The CAs measured with the powder coated sands all showed increases: the coarse, medium and fine sands had CAs of 123°, 124° and 128° corresponding to increases of 14°, 2° and 1° respectively compared to the simply silanised sands (Figure 4). These results indicate that the enhancement of CAs as a result of the powder coating procedure is dependent of the particle size of the sand, the coarser the sand, the greater the increase in hydrophobicity.

The effect of increasing *C* on the CA for a fixed mass mixing ratio of 1 to 1 was investigated next. When *C* was increased to 2*C* and 7*C*, a general increase in CA was recorded with the medium and fine sands (Figure 4b and c). However, with the coarse sand, there was comparatively no change in CA; the CAs measured at *C* and 7*C* being 123° and 122° respectively (Figure 4a). The amount of silica powder was then increased by raising the mass mixing ratio to 1 to 3. Despite a similar increase in CAs being observed with this new ratio compared to the simply silanised sand, increasing the mass of silica powder relative to the mass of sand did not further enhance the CAs of the powder-coated sands, e.g. with the coarse sand, the CA at concentration 2*C* at both mixing ratios was 120°.

4.2 Influence of silanisation and powder coating on particle size, particle shape and surface roughness

There was no measured change in particle size between the pure and silanised sands; the D_{50} of the sands were 768 µm for the coarse sand, 247 µm for the medium sand and 177 µm for the fine sand (Figure 5a, c and e). This indicates that the thickness of the PDMS coatings achieved on the silanised sands were less than the resolution of the lens in the DIA (10 µm). For the powder-coated sands, the coarse sand showed an increase in D_{50} as C increased. An increase of 88 µm as the coarse sands were powder-coated was observed at a concentration of 7C at the 1 to 1 mixing ratio when compared to the silanised sands (Figure 5a). With the medium and fine sands, the changes in D_{50} were close to the resolution of the lens in the DIA and insensitive to changes in C (Figure 5c and e). For instance, the D_{50} of the fine sand at the 1 to 1 mixing ratio were as follows: 169 µm (powder-coated at C), 177 µm (powder-coated at 2C) and 182 µm (powder-coated at 7C). An increase in fine content due to the silanised silica powder aggregating after the powder coating procedure was observed with the powder-coated medium and fine sands (Figure 5c and e), but not with the powder-coated coarse sand.

Similarly, a comparison of the median values of the shape parameters of the silanised and powder-coated sands show that regardless of particle size and mixing ratio, no change in particle shape was observed. Figure 5b, d and f illustrates the cumulative distributions of the three shape parameters for the hydrophilic, silanised and powder-coated sands at a 1 to 1 mixing ratio.

As for the effect of silanisation and powder coating on surface roughness, qualitative analysis of the sands obtained using the SEM microphotographs showed the adhered silica powders to the silanised sand (Figure 6a) while the optical white light profilometer was used to report quantitatively the surface roughness of the sands (Figure 6b and c). The R_a of the hydrophilic coarse, medium and fine sands were 559 nm, 621 nm and 689 nm respectively. The silanisation of the sands at a concentration of 0.53% resulted in an overall smoothening of the coarse (R_a = 477 nm), medium (R_a = 416 nm) and fine (R_a = 477 nm) sands due to the formation of the PDMS coating on the sands. These data suggest that besides molecular interactions such as Van der Waal forces occurring within the interface of the silanised sands and silanised silica powder, an increase in contact area (due to the smoothening of the sands) promotes adhesion.

This effect has been reported by Fuller and Tabor (1975) to influence adhesion; a decrease in surface roughness was shown to enhance adhesion. Powder coating the silanised sands resulted in an increase in R_a with all sands. Regardless of the mixing ratio, an increase in R_a as C increased to 2C and 7C was recorded. Compared to the silanised coarse sand (R_a = 477 nm), the R_a values of the powder-coated coarse sand at C, 2C and 7C at a 1 to 1 mixing ratio were 707 nm, 747nm and 840 nm respectively. However, when the mixing ratio switched from 1 to 1 to 1 to 3, R_a values became lower due to an increase in the silica powder adhered to the sands, causing the deviations of the asperities (silica powder) from the datum to diminish, thus leading to a decrease in R_a (Figure 7a and b).

4.3 Comparison of contact angles to theoretical models

According to equation (4), the ratio of cos θ_w to cos θ_y should equal the calculated ratio of actual to projected area of the solid, r, for the silanised and powder-coated sands to adhere to Wenzel's model. The silanised microscope slides were considered as ideal solids and θ_y taken as 103°. Because the roughness as characterised by the the optical white light profilometer cannot be translated into the roughness factor used in Wenzel's equation, r was calculated using the actual and projected areas from the 3D profiles generated with the optical white light profilometer. The effect of curvature was included in the measurements of the actual areas and r was obtained by dividing the actual area with the projected area (Figure 8). The plot of cos θ_w/cos θ_y versus r with θ_w equals to the experimentally measured CAs is shown in Figure 9. All data points lied above the unity line showing that cos θ_w/cos θ_y exceeded the r. These results demonstrate that because the silanisation and the powder coating procedure increases the values of CA and r, the water drops dispensed on the sands do not fully penetrate the surface protrusions. This suggests that the increases in CAs recorded with the silanised and powder-coated sands may not only be due to surface chemistry and surface roughness but also to the presence of air in between the water drops and the sands.

If using the Cassie-Baxter model (equation (5)) on the other hand, it is assumed that any change in hydrophobicity can only be linked to the surface chemistry and air, i.e. the influence of particle size, particle shape and surface roughness are not taken into account. From equation

(5), it can be deduced that increasing the area fraction of air in contact with the water drop, (1- f_1) leads to an increase in CA. Enhancements in CAs on flat surfaces have previously been attributed to (1- f_1), for example, Yu *et al*. (2019) illustrated that a rise in CA of 15° on hydrophobic glass surfaces compared to smooth surfaces was because of (1- f_1) increasing to 0.41. In our study, a similar value was obtained after the powder coating procedure with the coarse sands: the CA of the silanised sands was 109° and the resulting powder coating at 1 to 1 mixing ratio at *C* led to a CA of 123°. This corresponds to (1- f_1) equal to 0.13 and 0.41 for the silanised and powder-coated sands respectively. This means that for this sand, air occupies an additional 28% of area fraction when powder-coated.

The comparison with both theoretical models thus suggests that coating the sand particles with powder results in entrapment of air on the surface of the grains, contributing to enhance the hydrophobicity of the sand further than what is achieved by simple chemical treatment.

5. Conclusion

This paper presents a new methodology to optimise the hydrophobicity of granular materials by powder coating sands of variable sizes. The most significant enhancement in hydrophobicity as a consequence of the powder coating procedure was observed for the coarse sand, followed by the medium and fine sands. Compared to the silanised sands: 1) A maximum increase of 14° in CAs (from 109° to 123°) was recorded with the powder-coated sands. 2) There was no change in particle shape recorded when the sands were powder-coated. 3) An increase in particle size was observed only with the coarse sand whereas the medium and fine sands showed only increases in the fines content. 4) The surface roughness of all sands increased. The concept of physically modifying granular materials to tune hydrophobicity can potentially be extended to a wide variety powders of different shapes and of finer sizes (e.g. nanosilica) for their eventual deployment in ground engineering.

Acknowledgements

This work was supported by the General Research Fund (Grant 17203417) from the Research Grants Council of Hong Kong Special Administrative Region, China.

References

Bachmann, J., Ellies, A. and Hartge, K. (2000) Development and application of a new sessile drop contact angle method to assess soil water repellency. *J. Hydrol.* **231-232**: 66-75.

Bachmann, J., Woche, S. K., Goebel, M. O., Kirkham, M. B. and Horton, R. (2003) Extended methodology for determining wetting properties of porous media. *Water resources research* **39(12)**.

Bachmann, J. and McHale, G. (2009) Superhydrophobic surfaces: a model approach to predict contact angle and surface energy of soil particles. *Eur. J. Soil Sci.* **60(3)**: 420-430.

Bardet, J., Jesmani, M., Jabbari, N. and Lourenco, S. D. N. (2014) Permeability and compressibility of wax-coated sands. *Geotechnique* **64(9)**: 752-755.

Bentz, D. P., Ferraris, C. F., Jones, S. Z., Lootens, D. and Zunino, F. (2017) Limestone and silica powder replacements for cement: Early-age performance. *Cem. Concr. Compos.* **78**: 43-56.

Blossey, R. (2003) Self-cleaning surfaces—virtual realities. *Nat. Mater.* **2(5)**: 301.

Brown, H.R. (2000) Polymer adhesion. *Mater. Forum.* **24**: 49-58.

Camino, G., Lomakin, S. M. and Lazzari, M. (2001) Polydimethylsiloxane thermal degradation Part 1. Kinetic aspects. *Polymer* **42(6)**: 2395-2402.

Carrillo, M. L. K., Yates, S. R. and Letey, J. (1999) Measurement of initial soil-water contact angle of water repellent soils. *Soil Sci. Soc. Am. J.* **63(3)**: 433-436.

Cassie, A. B. D. and Baxter, S. (1944) Wettability of porous surfaces. *Trans. Faraday Soc.* **40**: 546-551.

Chan, C. S. H. and Lourenço, S. D. N. (2016) Comparison of three silane compounds to impart water repellency in an industrial sand. *Geotechnique Lett.* **6(4)**: 263-266.

Darmanin, T. and Guittard, F. (2015) Superhydrophobic and superoleophobic properties in nature. *Mater. Today* **18(5)**: 273-285.

Dekker, L. W. and Ritsema, C. J. (1994) How water moves in a water repellent sandy soil: 1. Potential and actual water repellency. *Water Resour. Res.* **30(9)**: 2507-2517.

Doerr, S. H., Shakesby, R. A. and Walsh, R. P. D. (2000) Soil water repellency: its causes, characteristics and hydro-geomorphological significance. *Earth-Sci. Rev.* **51(1-4)**: 33-65.

Dong, Y. and Pamukcu, S. (2015) Thermal and electrical conduction in unsaturated sand controlled by surface wettability. *Acta Geotechnica* **10(6):** 821-829.

Feng, L., Li, S., Li, Y., Li, H., Zhang, L., Zhai, J., Song, Y., Liu, B., Jiang, L. and Zhu, D. (2002) Super-hydrophobic surfaces: from natural to artificial. *Adv. Mater.* **14(24)**: 1857-1860.

Fuller, K. N. G. and Tabor, D. (1975) The effect of surface roughness on the adhesion of elastic solids. *Proceedings of the Royal Society A: Mathematical, Physical and Engineering Sciences.* **345(1642)**: 327-342.

Goebel, M.-O., Woche, S. K., Bachmann, J., Lamparter, A. and Fischer, W. R. (2007) Significance of wettability-induced changes in microscopic water distribution for soil organic matter decomposition. *Soil Sci. Soc. Am. J.* **71(5)**: 1593-1599.

Grunze, M. (1999) Driven liquids. *Science* **283(5398)**: 41-42.

Hernandez, J., Vargas, S., Estévez, M., Vázquez, G., Zepeda, A. and Rodríguez, R. (2005) Hydrophobic modification of an expansive soil using polymers and organic compounds: a comparative study with lime. *Geotechnique* **55(8)**: 613-616.

Keatts, M.I., Daniels, J.L., Langley, W.G., Pando, M.A. and Ogunro, V.O. (2018) Apparent Contact Angle and Water Entry Head Measurements for Organo-Silane Modified Sand and Coal Fly Ash. *J. Geotech. Geoenviron. Eng.* **144(6)**: 04018030.

Kim, D., Yang, H., Kim, K. and Yun, T. (2015) Experimental investigation of evaporation and drainage in wettable and water-repellent sands. *Sustainability*, **7(5)**: 5648-5663.

Kinloch, A. J. (1980) The science of adhesion. *J. Mater. Sci.* **15(9)**: 2141-2166.

Lafuma, A. and Quéré, D. (2003) Superhydrophobic states. *Nat. Mater.* **2(7)**: 457-460.

Lee, C., Yang, H. J., Yun, T. S., Choi, Y. and Yang, S. (2015) Water-entry pressure and friction angle in an artificially synthesized water-repellent silty soil. *Vadose Zone J.* **14(4)**.

Liu, D., Lourenço, S.D.N and Yang, J. (2019) Critical state of polymer-coated sands. *Geotechnique* 1-6.

Ng, S. H. Y. and Lourenco, S. D. N. (2016) Conditions to induce water repellency in soils with dimethyldichlorosilane. *Geotechnique* **66(5)**: 441-444.

Orozco, L.F. and Caicedo, B. (2017) Water migration in unsaturated partially hydrophobic soils. *Geotechnique Lett*. **7(1)**: 18-23.

445 Saulick, Y., Lourenço, S. D. N. and Baudet, B. A. (2017) A semi-automated technique for
446 repeatable and reproducible contact angle measurements in granular materials using the
447 sessile drop method. *Soil Sci. Soc. Am. J.* **81(2)**: 241-249.
448 Saulick, Y., Lourenço, S. D. N., Baudet, B. A., Woche, S. K. and Bachmann, J. (2018) Physical
449 properties controlling water repellency in synthesized granular solids. *Eur. J. Soil Sci.* **69(4)**:
450 698-709.
451 Shirtcliffe, N. J., McHale, G., Newton, M. I., Chabrol, G. and Perry, C. C. (2004) Dual-scale
452 roughness produces unusually water-repellent surfaces. *Adv. Mater.* **16(21)**: 1929-1932.
453 Subedi, S., Kawamoto, K., Jayarathna, L., Vithanage, M., Moldrup, P., Wollesen De Jonge, L.
454 and Komatsu, T. (2012) Characterizing time-dependent contact angles for sands
455 hydrophobized with oleic and stearic acids*. Vadose Zone J.***11(1)**.
456 Tripp, C. and Hair, M. (1991) Reaction of chloromethylsilanes with silica: a low-frequency
457 infrared study. *Langmuir* **7(5)**: 923-927.
458 Wang, Z., Koratkar, N., Ci, L. and Ajayan, P. (2007) Combined micro-/nanoscale surface
459 roughness for enhanced hydrophobic stability in carbon nanotube arrays. *Appl. Phys. Lett.*
460 **90(14)**: 143117.
461 Wenzel, R. N. (1936) Resistance of solid surfaces to wetting by water. *Ind. Eng. Chem.* **28(8)**:
462 988-994.
463 Yang, H., Baudet, B. A. and Yao, T. (2016) Characterization of the surface roughness of sand
464 particles using an advanced fractal approach. *Proceedings of the Royal Society A:*
465 *Mathematical, Physical and Engineering Sciences* **472(2194)**.
466 Young, T. (1805) An essay on the cohesion of fluids. *Philos. Trans. R. Soc. London* **95**: 65-87.
467 Yu, L., Kang, Y., Tang, H. and Zhou, J. (2019) Functionalization of Commercial Sand Core
468 Funnels as Hydrophobic Materials with Novel Physicochemical Properties. *ACS Appl. Mater.*
469 *Interfaces.* **11(7)**: 7510-7521.
470 Zhang, P., Wang, S., Wang, S. and Jiang, L. (2015) Superwetting surfaces under different
471 media: Effects of surface topography on wettability. *Small* **11(16)**: 1939-1946.
472 Zhang, H. Y., Zhu, S. B., Li, M. and Zhang, X. C. (2016) Water repellency of monument soil
473 treated by tung oil. *Geotech Geol Eng.* **34(1)**: 205-216.

474 Zimmermann, J., Reifler, F. A., Fortunato, G., Gerhardt, L. C. and Seeger, S. (2008) A simple,
475 one-step approach to durable and robust superhydrophobic textiles. *Adv. Funct. Mater.*
476 **18(22)**: 3662-3669.
477

Figure captions

Figure 1. Schematic representation of a drop of water (a) on an ideal flat solid; (b) in the Wenzel state and (c) in the Cassie-Baxter state

Figure 2. Schematic representation of the optimisation of hydrophobicity of sands

Figure 3. Relationship between concentration of dimethyldichlorosilane and contact angles for the coarse sand, medium sand, fine sand and silica powder

Figure 4. Comparison of contact angles of powder-coated sands to silanised sands for different mass mixing ratios: (a) coarse, (b) medium and (c) fine sands. *C*, 2*C* and 7*C* refer to the concentrations at which the sands were initially chemically modified before powder coating. Inset photographs show 10µL water drops on the silanised sands compared to the powder-coated sands in at a mixing ratio of 1 to 1

Figure 5. Characterisation using dynamic image analyser: particle size distributions of (a) coarse, (c) medium, (e) fine sands and particle shape distributions of (b) coarse, (d) medium, (f) fine sands at a mixing ratio of 1 to 1

Figure 6. (a) SEM microphotographs showing the silanised and powder-coated coarse sands at similar magnifications; (b) optical white light profilometry images of the silanised (left) and powder-coated (right) coarse sands; (c) 2D profiles extracted from the optical white light profilometry images

Figure 7. Change in surface roughness as the sands are powder-coated in a mixing ratio of (a) 1 to 1 and (b) 1 to 3. *C*, 2*C* and 7*C* refer to the concentrations at which the sands were initially chemically modified before powder coating

Figure 8. (a) Projected and (b) actual areas of a powder-coated sand

Figure 9. Comparison of the ratio of contact angles to the roughness factor, *r* for the (a) coarse (b) medium and (c) fine sands. The values of θ_w and θ_y are the experimentally measured contact angles on the sands (silanised and powder-coated) and the silanised microscope slides respectively

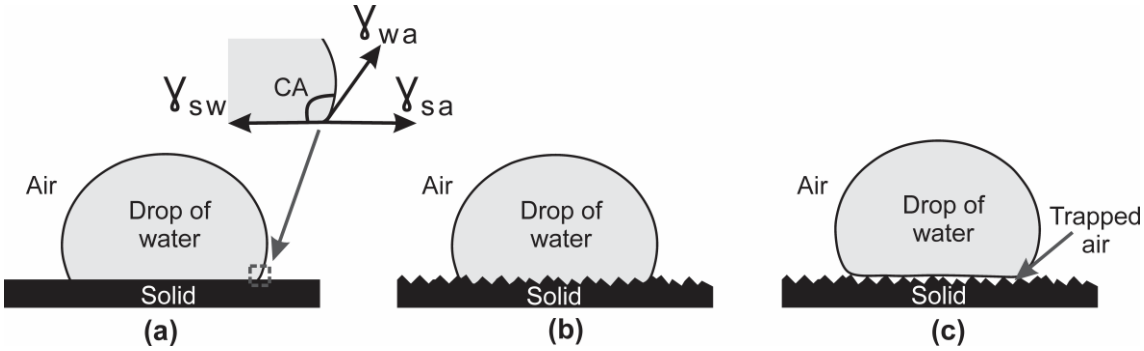

Figure 1. Schematic representation of a drop of water (a) on an ideal flat solid; (b) in the Wenzel state and (c) in the Cassie-Baxter state

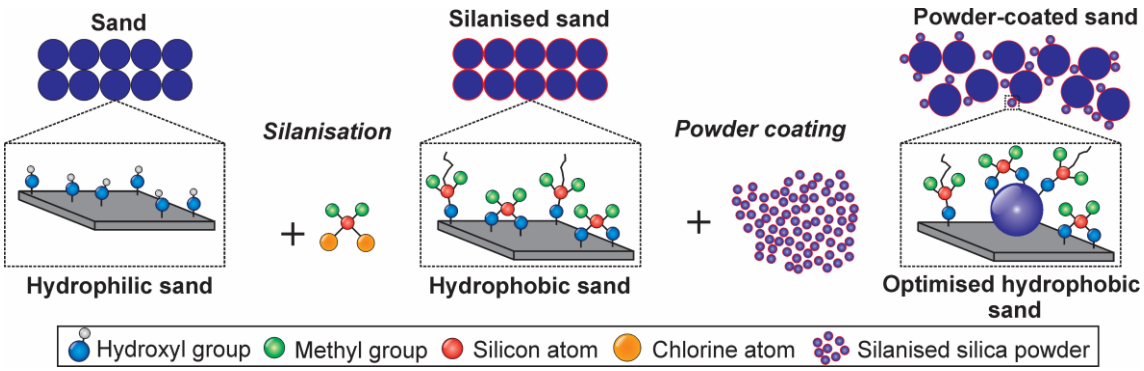

Figure 2. Schematic representation of the optimisation of hydrophobicity of sands

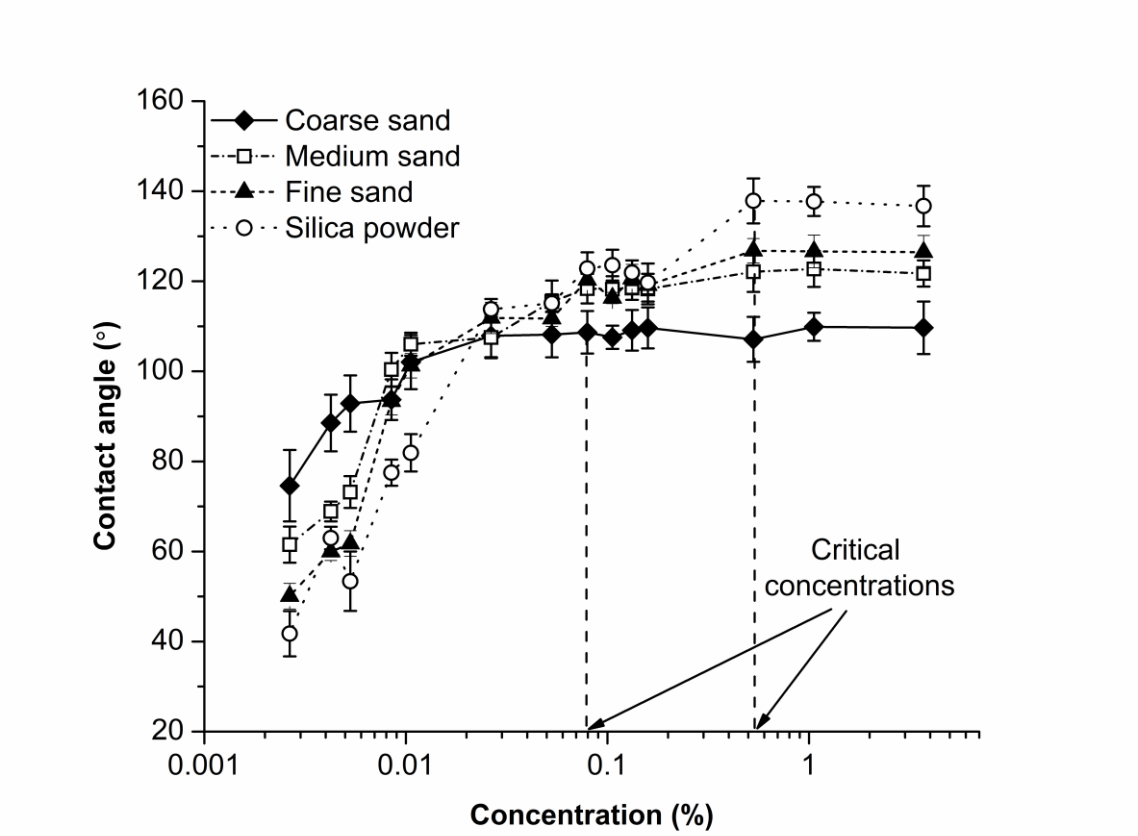

Figure 3. Relationship between concentration of dimethyldichlorosilane and contact angles for the coarse sand, medium sand, fine sand and silica powder

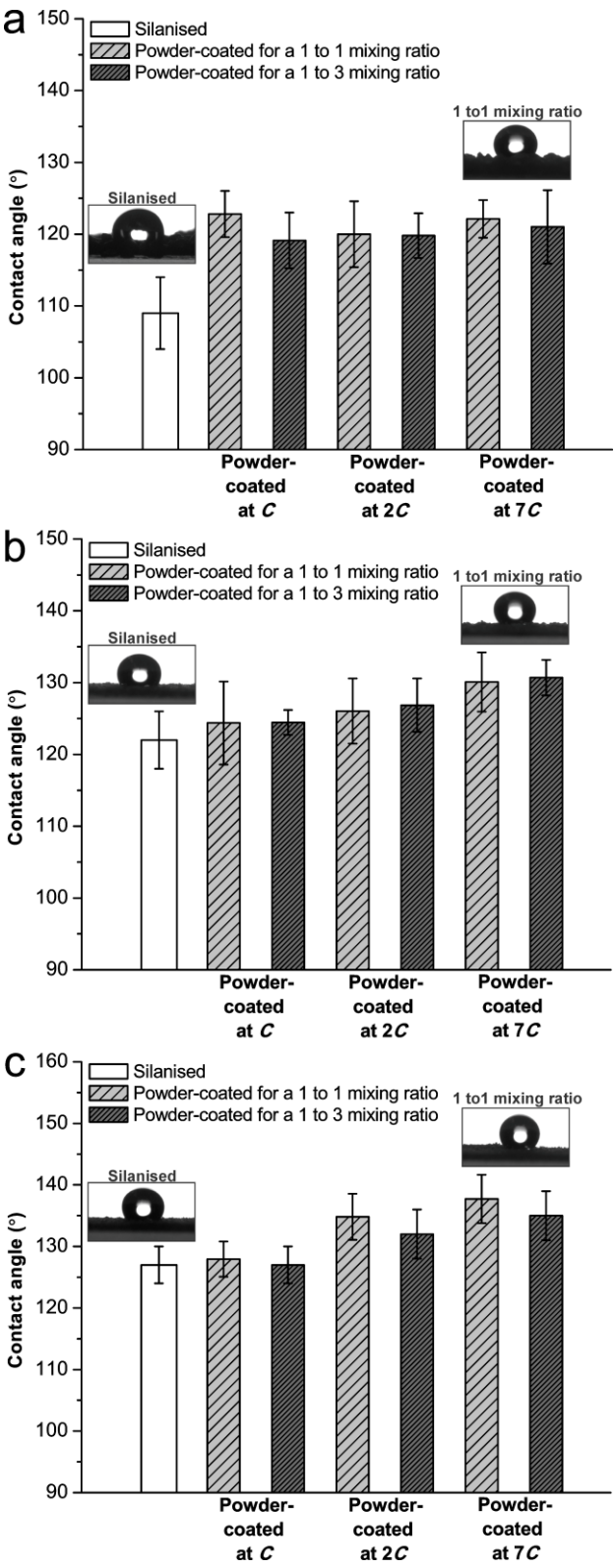

Figure 4. Comparison of contact angles of powder-coated sands to silanised sands for different mass mixing ratios: (a) coarse, (b) medium and (c) fine sands. *C*, 2*C* and 7*C* refer to the concentrations at which the sands were initially chemically modified before powder coating. Inset photographs show 10µL water drops on the silanised sands compared to the powder-coated sands in at a mixing ratio of 1 to 1

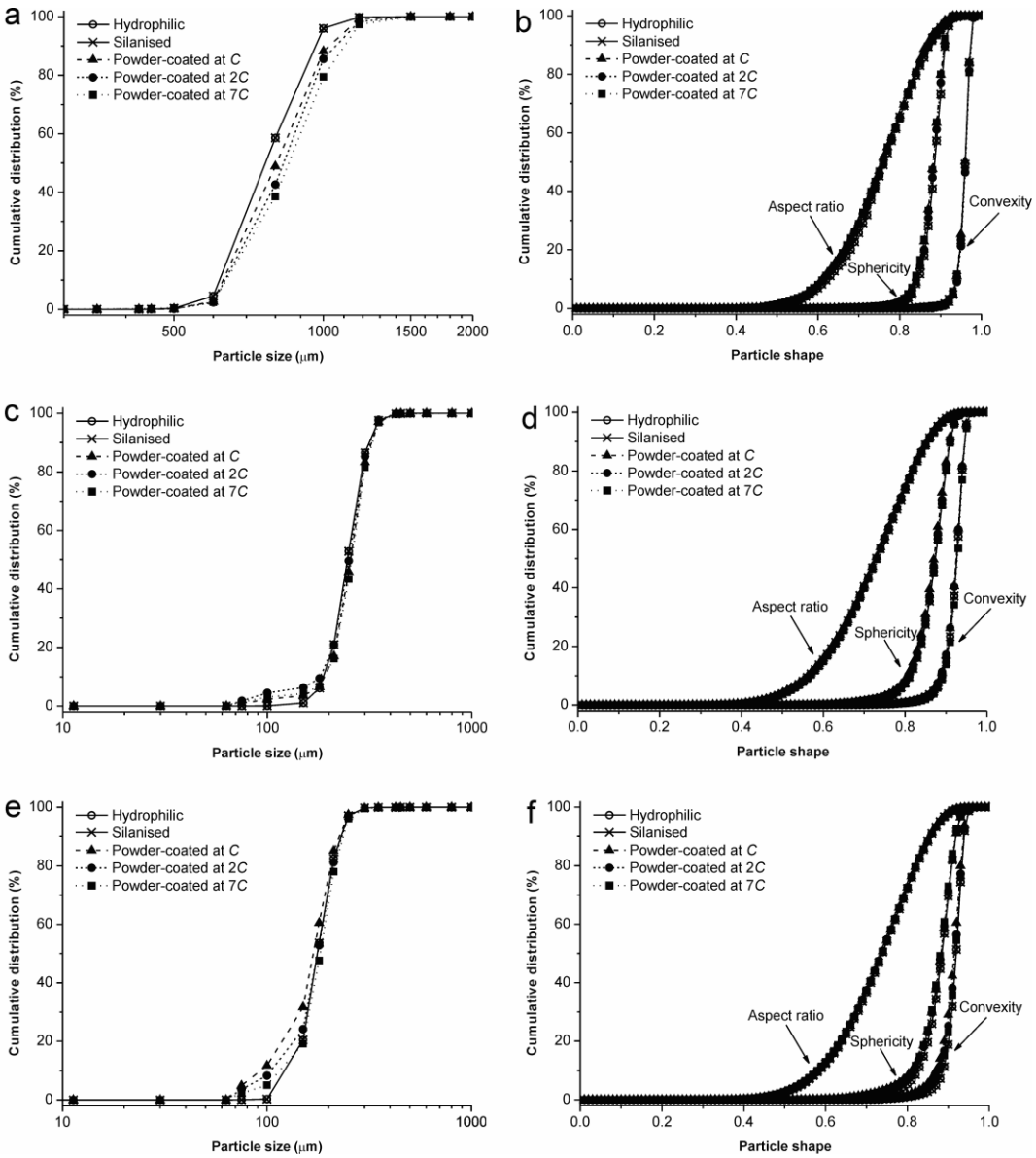

Figure 5. Characterisation using dynamic image analyser: particle size distributions of (a) coarse, (c) medium, (e) fine sands and particle shape distributions of (b) coarse, (d) medium, (f) fine sands at a mixing ratio of 1 to 1

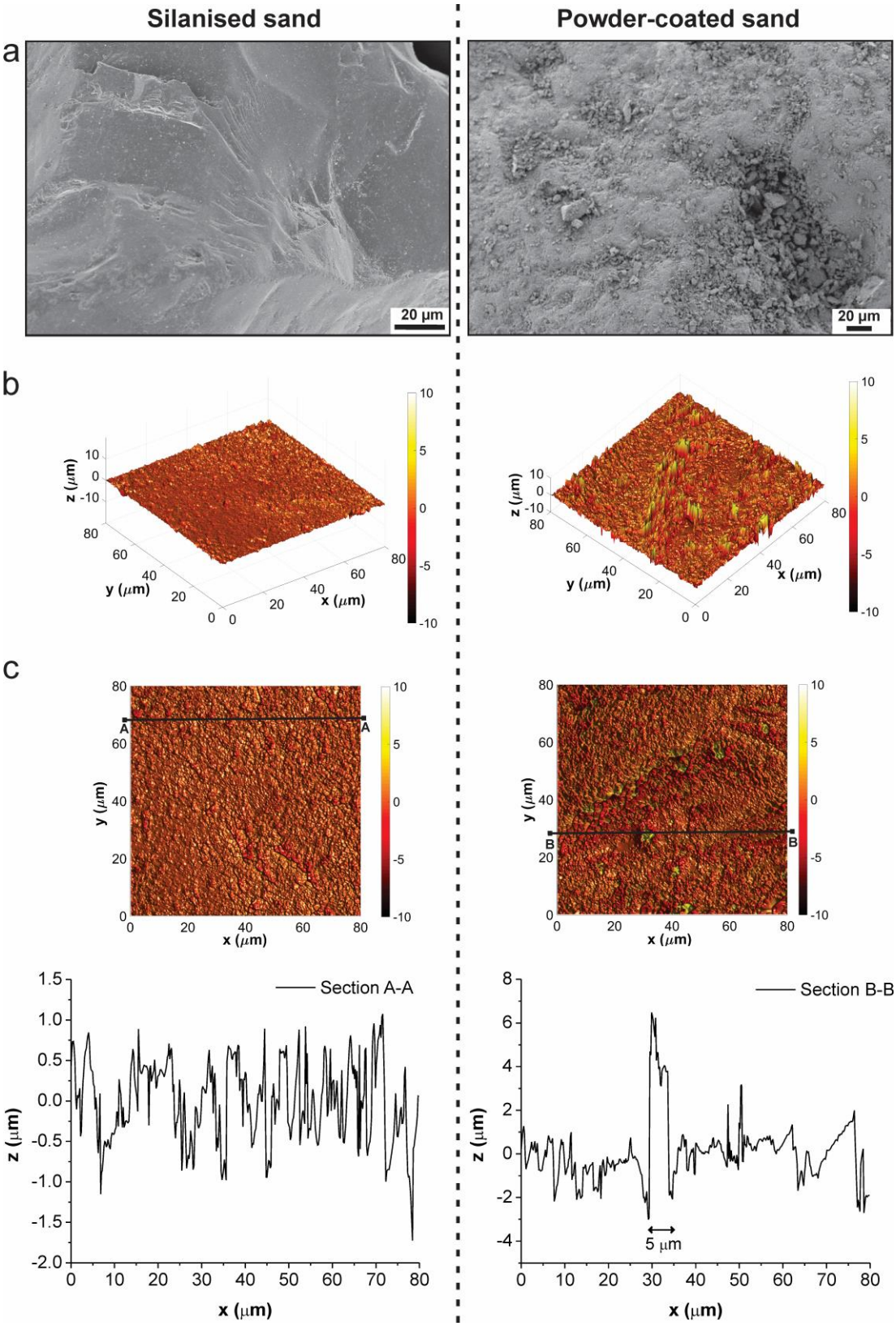

Figure 6. (a) SEM microphotographs showing the silanised and powder-coated coarse sands at similar magnifications; (b) optical white light profilometry images of the silanised (left) and powder-coated (right) coarse sands; (c) 2D profiles extracted from the optical white light profilometry images

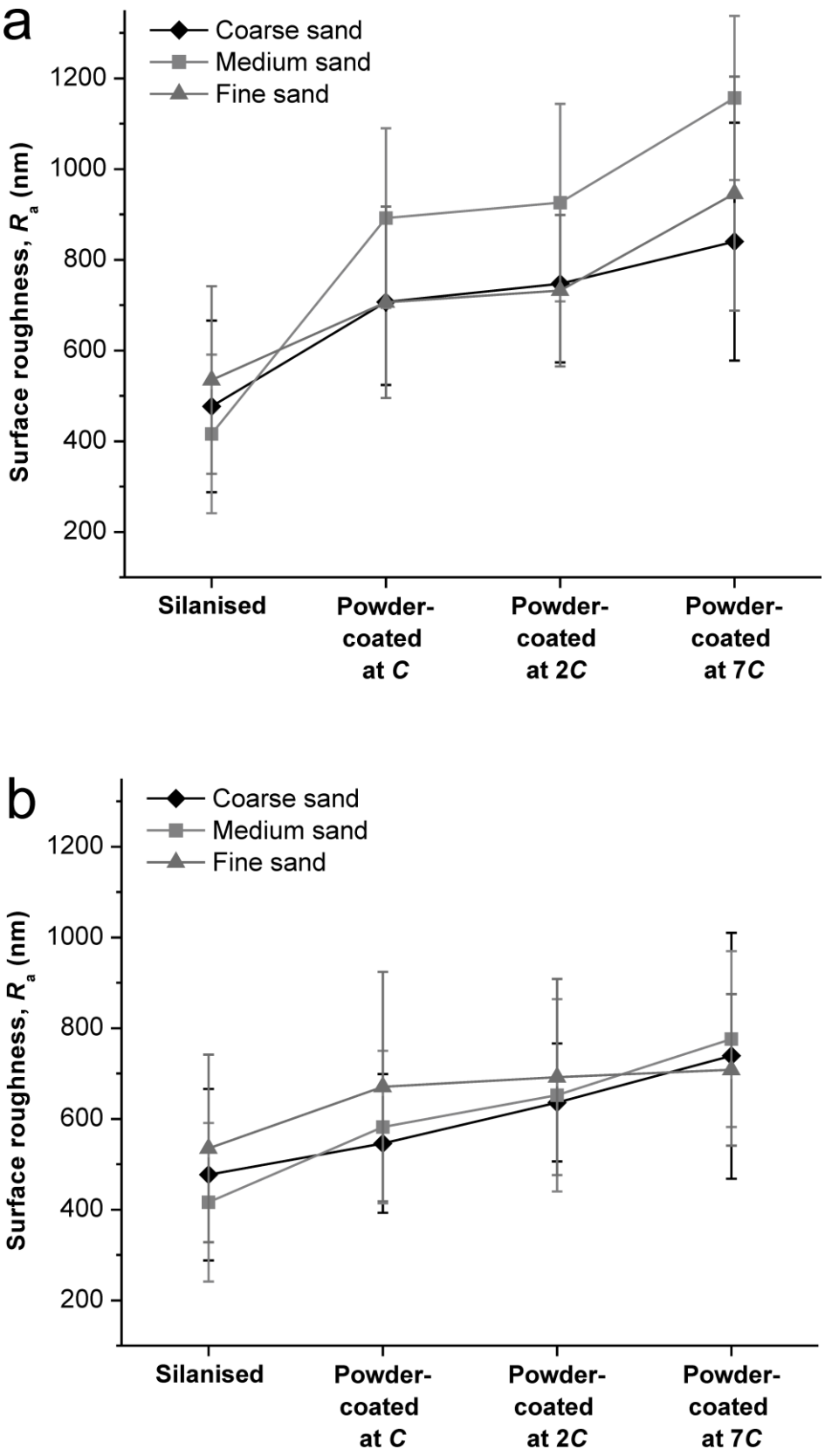

Figure 7. Change in surface roughness as the sands are powder-coated in a mixing ratio of (a) 1 to 1 and (b) 1 to 3. *C*, 2*C* and 7*C* refer to the concentrations at which the sands were initially chemically modified before powder coating

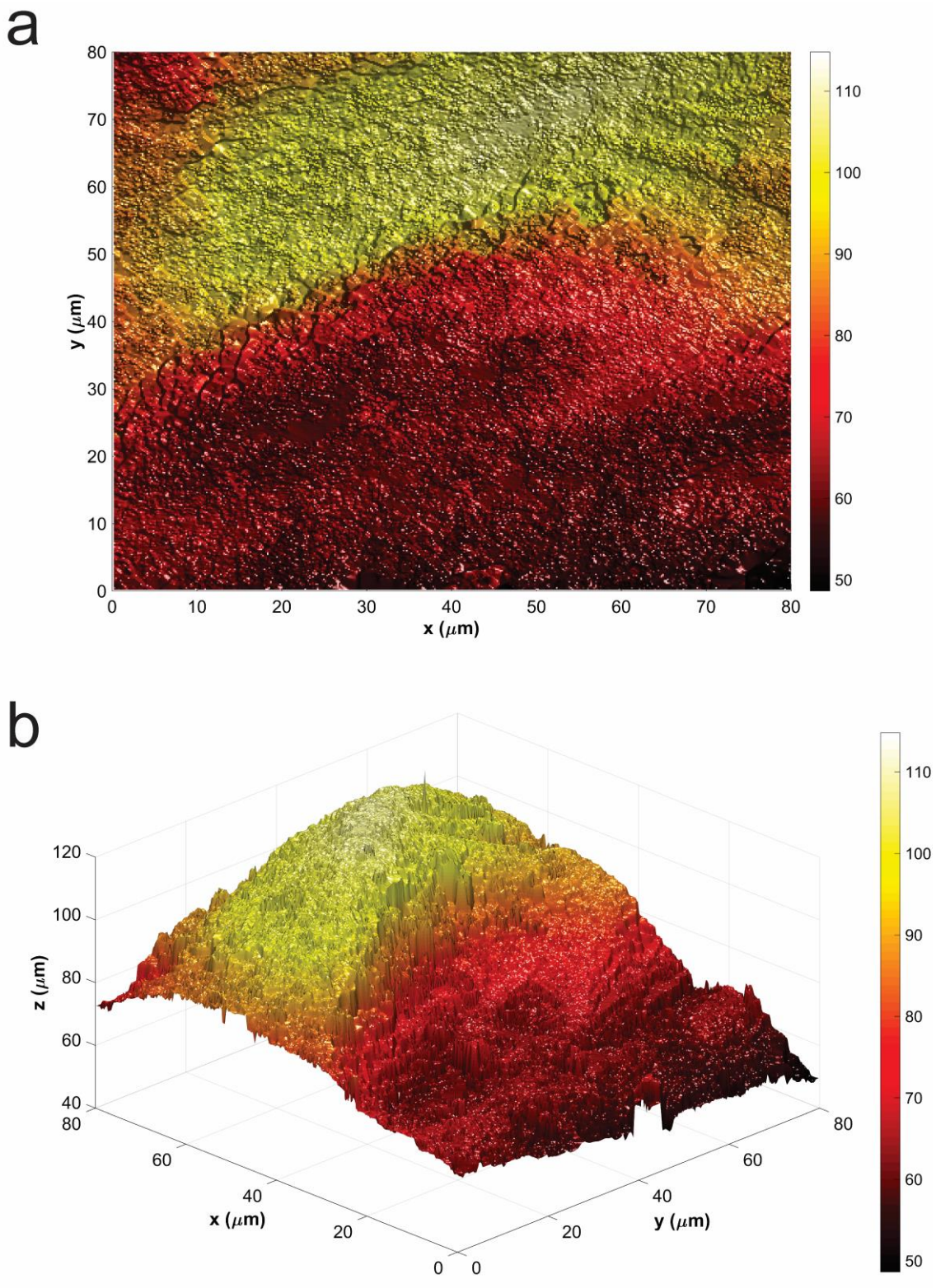

Figure 8. (a) Projected and (b) actual areas of a powder-coated sand

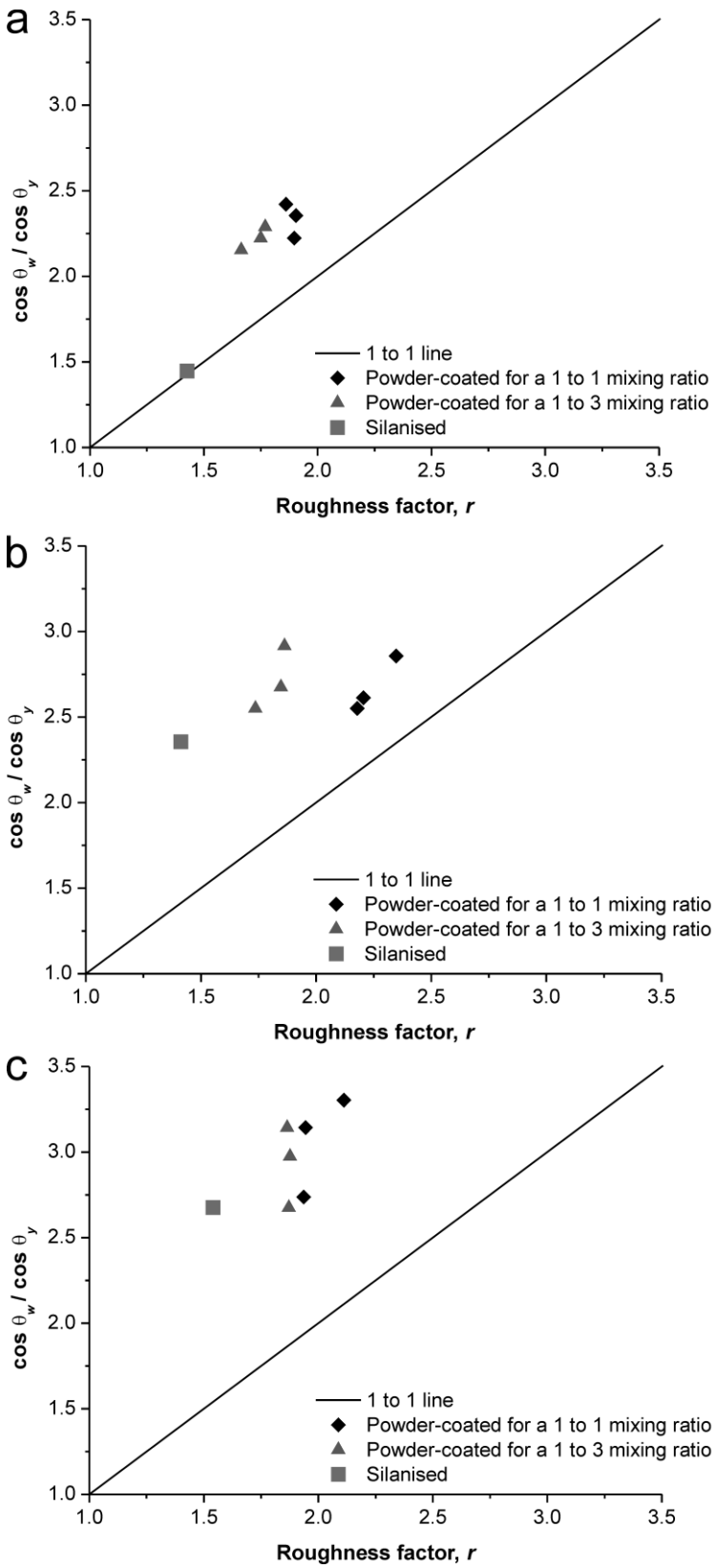

Figure 9. Comparison of the ratio of contact angles to the roughness factor, *r* for the (a) coarse (b) medium and (c) fine sands. The values of θ_w and θ_y are the experimentally measured contact angles on the sands (silanised and powder-coated) and the silanised microscope slides respectively